

**SINTERING STUDIES OF ZIRCONIA-YTTRIA SOLID ELECTROLYTES
BY SCANNING ELECTRON MICROSCOPY AND
IMPEDANCE SPECTROSCOPY ANALYSIS**

R. Muccillo¹, D. Z. de Florio², E. N. S. Muccillo¹

Centro Multidisciplinar para o Desenvolvimento de Materiais Cerâmicos

¹CCTM - IPEN, C.P. 11049, Pinheiros

S. Paulo, SP, Brazil 05422-970

²Instituto de Química, UNESP, R. Prof. Francisco Degni s/n

Araraquara, SP, Brazil 14801-970

muccillo@usp.br

ABSTRACT

A set of cold-pressed $ZrO_2:8\text{mol}\%Y_2O_3$ (Yttria Fully-Stabilized Zirconia, Y-FSZ) specimens, using sub-micron sized powders, was pre-sintered to 70% of the full density, followed by sintering at different times at low temperatures (two-step sintering). The sintering temperature was chosen after dilatometric measurements in the range room temperature-1500 °C. All specimens were analyzed by impedance spectroscopy measurements at a temperature low enough to inhibit grain growth, and by scanning electron microscopy after polishing and thermally etching, to evaluate average grain sizes. Another set of Y-FSZ specimens was sintered for different times at a temperature corresponding to the third sintering stage, to promote grain growth without shrinkage. The grain boundary resistivity decreases for increasing sintering time in agreement with the elimination of interfaces during grain growth. The results on two-step sintering show that the second-step isothermal sintering always results in increase of the average grain size for increasing sintering times irrespective of the sintering stage.

Keywords: sintering, grain growth, impedance spectroscopy

INTRODUCTION

Based on the assumption that capillary driving forces for sintering (involving surfaces) and grain growth (involving grain boundaries) have approximately the same magnitude, suppression of the final stage grain growth is achieved by exploiting the difference in kinetics between grain boundary diffusion and grain boundary migration [6]. Results have been presented for obtaining fully dense cubic Y_2O_3 with 60 nm average grain size by a simple two-step sintering, firstly at 1310 °C and secondly at 1150 °C without applied pressure, remembering that Y_2O_3 melts at a very high temperature (2,439 °C). The proposed "recipe" for cost-effective preparation of nanocrystalline materials for practical applications was: first step sintering for a short time (to avoid grain growth) at a temperature for reaching a density of 70% of the theoretical density (T.D.) and a second step sintering for a long time at a temperature low enough to densify the specimen without grain growth [6]. Recently the feasibility of densification without grain growth by two-step sintering was tested in liquid phase sintering of silicon carbide ceramics [17]. Finally, dense nanostructured ceramics were obtained. Yttria-stabilized zirconia in the cubic fluorite structural phase is one of the most studied ceramic materials due to its behavior as solid electrolyte. It is an oxide ion conductor due to the extrinsic oxide-ion vacancies promoted by the incorporation of Y^{3+} ions substitutionally in the ZrO_2 lattice. This solid electrolyte is used in Solid Oxide Fuel Cells, which are devices for the production of environmental clean energy [12]. As most of the properties of YSZ ceramics have been studied in full, this solid electrolyte may be considered a model of a solid electrolyte for basic research work. Moreover, it is commercially available with high degree of purity and/or with full chemical analysis. Zirconia-based ceramics are also widely used as electrochemical transducers in oxygen sensors [12]. Some of the requirements for using these ceramics in sensor devices are high density and reproducibility of the electrical properties. Hence, the sintering process, whereby interparticle pores in a granular material are eliminated by atomic diffusion driven by capillary forces [9], has to be well controlled in manufacturing the ceramic bodies. Sintering can be described briefly as the phenomenon that occurs during heating up green compacts leading to pore elimination associated to grain growth and providing well defined grain boundaries [9]. There is basically the conversion of a large number of small particles in a lower number of larger particles, that is, grain growth and solid-solid interfaces substitution for higher energy gas-solid interfaces. In most cases this is accompanied by densification. The geometric variation of the ceramic dimensions associated to sintering follows three stages: the initial stage with particles forming bonds at the particle contacts; the intermediate stage with the smoothing of the pore structure; and the final stage corresponding to closed spherical pores that shrink slowly by vacancy diffusion to grain boundaries [9, 5]. Several processes are known to occur during sintering, the solid state sintering being the most important in zirconia ceramics manufactured for mechanical, electrical and optical applications. In this case, the main sintering process involves no liquid phase formation, i.e., all constituents of the powder compacts stay in the solid state [21]. For high temperature applications, for example as solid electrolyte in sensors for determining oxygen content in molten steels (~ 1600 °C), a ceramic material with low grain size would be expected to have better thermal shock resistance properties. Moreover, a sintering procedure leading to full density ceramic pieces

without using for a long time temperatures higher than approximately 1100 °C would be useful for co-sintering the cathode oxide-electrolyte oxide SOFCs assembly preventing the undesirable reaction between the two oxides, known to degrade the performance of those devices [23].

We have then decided to perform experimental work in that material to check the two-step sintering process for obtaining high density with low average grain size specimens. The experimental sequence was: 1) to carry out dilatometric measurements to look for the suitable temperature for preparing approximately 70%T.D. specimens; 2) to follow the two-step sintering by choosing different second-step temperatures for preparing several specimens for different sintering times; 3) to observe the surfaces of the specimens in the scanning electron microscope; and finally, 4) to study the electrical behavior of all specimens by the electrochemical impedance spectroscopy technique.

Thirty-five years ago the complex admittance technique was applied for the first time to a solid electrolyte, $(\text{ZrO}_2)_{0.9}(\text{Y}_2\text{O}_3)_{0.1}$ [3]. The electrical conductivity of polycrystalline ceramics has been shown extensively to have two main components: bulk or intragranular conductivity and internal surfaces or grain boundary conductivity. The former depends on the grain mobility of charge carriers, while the latter on the blocking of charge carriers, mainly at grain boundaries. Grain boundary conductivity may be decreased by the blocking of charge carriers by other microstructure defects like pores or insulating second phase inclusions, these defects being called "blockers" [8]. Mobile charge carriers either can permeate freely through grain boundaries or be blocked at certain grain boundary locations. Two blocking parameters have been proposed to help the analysis of charge transport in solid electrolytes [13, 14]: the resistance blocking factor α_R and the frequency factor α_f . The resistance blocking factor, defined as the relative amount of charge carriers that are blocked at grain boundaries, is determined simply by dividing the grain boundary resistivity by the total resistivity, and these values are taken from the $(-Z'' \times Z')$ impedance diagrams. The resistance blocking factor α_R is a characteristic parameter related to the contact between grains and can be associated to grain boundary density. The grain boundary density is already known to be related to the specimen average grain size [14, 22]. Here will be taken into account that α_R is proportional to the equivalent blocker area normal to the electric field. Or simply, in other words, α_R is proportional to the average surface between grains, i.e., the average intergranular surface. The other blocking parameter, the frequency factor, is defined as the ratio of the characteristic frequency of the grain boundary resistivity to that of the grain resistivity. The characteristic frequencies are the apex frequencies in the semicircles in the $(-Z'' \times Z')$ impedance diagrams. It has been shown that α_f is proportional to the average blocker thickness or to the average intergranular distance, i.e. to the average pore thickness. The product of both resistance blocking factor and frequency factor ($\alpha_R \cdot \alpha_f$) is then proportional to the volume between grains, i.e. to the pore volume [14]. Results on impedance spectroscopy of zirconia ceramics as a function of sintering parameters have been reported [14-10]. Conductivity measurements with current of variable frequency taken in zirconia-yttria solid electrolytes with different average grain sizes showed that the bulk (grain) conductivity does not depend on grain size while the grain boundary conductivity does [2, 10, 7]. Specimens with different grain sizes were obtained by firing hot-pressed samples at different temperatures up to 2000 °C. The effect of microstructure on zirconia-yttria conductivity, using the impedance spectroscopy technique has been reported, showing that the higher is the average grain

size, the lower is the grain boundary resistivity, the bulk resistivity remaining constant [11, 24]. The densification process of barium titanate has also been studied by impedance spectroscopy [19]. A correlation has been found between the activation energies of grain and grain boundary conductivities and the density after sintering. Recently it has been proposed that dense nanocrystalline ceramics could be obtained without final-stage grain growth if a special two-sintering step procedure is followed [6].

Usually sintering is monitored by density or shrinkage measurements. There are some reports in the literature on the application of the impedance spectroscopy technique to study sintering of ceramic solid electrolytes [22, 7] and glasses [20]. The idea is that the modifications of interfaces in either crystalline or amorphous solid dielectrics, like sintering due to pore elimination can be analyzed by measuring the electrical resistivity of the interfaces. The separation of bulk resistivity and grain boundary resistivity in the frequency domain by impedance spectroscopy offers the possibility of using that technique for following sintering processes. In this paper, the two-step sintering process is applied to produce zirconia-8 mol% yttria dense samples. The impedance spectroscopy and the traditional scanning electron microscopy technique are used to determine parameters for studying sintering of zirconia ceramics. Even though further experimental work is required at other different temperature profiles, the results here presented show that the two-step sintering is not effective for inhibiting grain growth in these ceramics, which are known to be one of the most used commercial ceramics for application in ceramic sensors as well as in Solid Oxide Fuel Cells.

MATERIALS AND METHODS

ZrO₂:8% mol Y₂O₃ was a commercial powder from Tosoh, Japan. Phase analysis was evaluated by X-ray diffraction with a Bruker-AXS D8 Advance diffractometer. Linear shrinkage measurements upon heating were carried out in a Netzsch DIL402E/7 dilatometer. Sample pellets 10 mm diameter and 2 mm thickness were prepared by uniaxially at 100 MPa followed by isostatically pressing at 200 MPa. The electroding of the planar opposite surfaces of the pellets were done by painting with silver paste and firing at 400 °C. The samples, three at a time, were inserted into a homemade (alumina and inconel 600 frames, platinum leads) sample chamber and positioned inside a tubular furnace. Platinum electrodes connected the painted surfaces of the specimen to an HP4192A LF Impedance analyzer controlled by a model 362 Hewlett Packard Controller for collecting, storing and processing $[-Z''(\omega) \times Z'(\omega)]$ data in the 5 Hz - 13 MHz frequency range. The applied voltage signal amplitude was 100 mV. A K-type thermocouple with its tip located close to the samples was used for temperature monitoring. The analysis of the $[-Z''(\omega), Z'(\omega)]$ impedance spectroscopy diagrams were done in the frequency domain [15]. Samples for observation in a scanning electron microscope were polished with diamond paste (30-to-3 microns grades). The grain morphology of polished surfaces of the sintered pellets was observed in a LEO 440I Oxford scanning electron microscope. The determination of the average grain sizes on the amplified micrographs obtained by SEM was done according to the method proposed by Mendelson [18] and available commercial software.

RESULTS AND DISCUSSION

Figure 1 shows the linear shrinkage of green pellets of zirconia-8 mol% yttria ceramics in the temperature range room temperature-1500 °C, for a 10 °C min⁻¹ heating rate. The temperature range measured for the first stage of sintering, where no appreciable shrinkage is detected, is room temperature-~1000 °C. After reaching that temperature, fast shrinkage starts and the specimen thickness decreases about 18 % at 1500 °C.

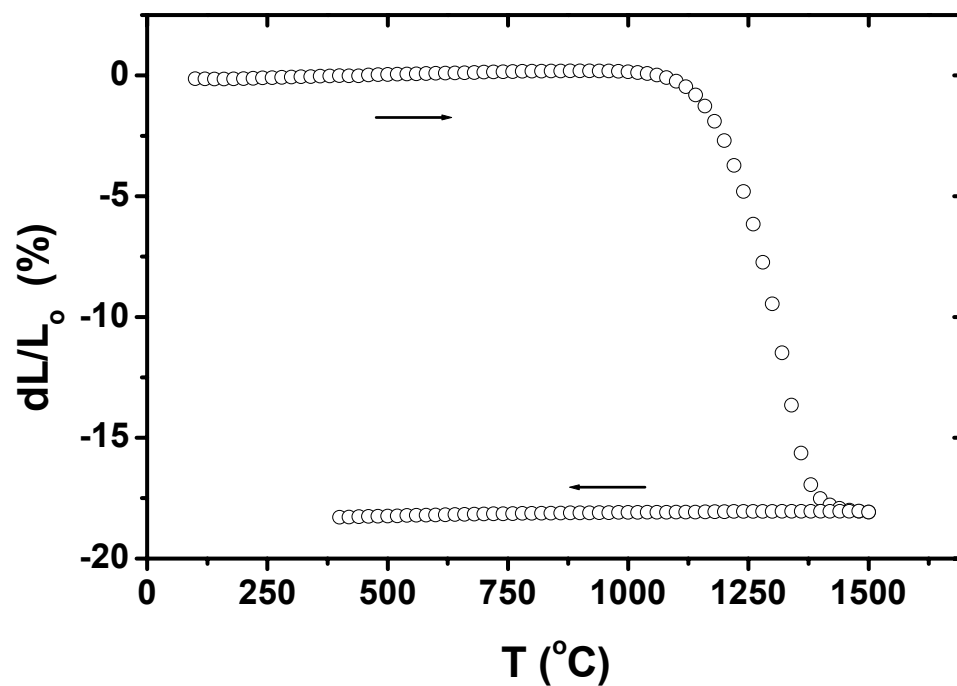


Figure 1: Linear shrinkage of a green pellet of ZrO₂:8 mol% Y₂O₃ in the temperature range room temperature - 1500 °C.

Impedance diagrams of ZrO₂:8% mol Y₂O₃ as a function of sintering time at 1350 °C are shown in Fig. 2. All measurements were performed at 400 °C. Two semicircles are easily resolved: one at high frequencies due to the contribution of the ceramic grains and the other due to the contribution of grain boundaries to the electrical resistivity [4, 16]. The data at frequencies below approximately 100 Hz belong to the electrode polarization. As expected, the larger is the sintering time at 1350 °C, the smaller is the diameter of the semicircle due to the grain boundaries, no variation being detected in the diameter of the semicircle due to charge transport inside the grains [7]. The impedance diagrams showing the increase of the average grain size as a function of the isothermal sintering time may then be used to follow grain growth.

The semicircle arcs in the impedance diagrams due to grains (intragranular contribution) do not change for different sintering times at 1350 °C. The semicircle arc due to grain boundary contributions, on the other hand, decreases for increasing sintering times. These results, after data

deconvolution, are plotted in Fig. 3. The intergranular resistance decreases as the density of the intergranular surfaces decreases due to the increase in the average grain size.

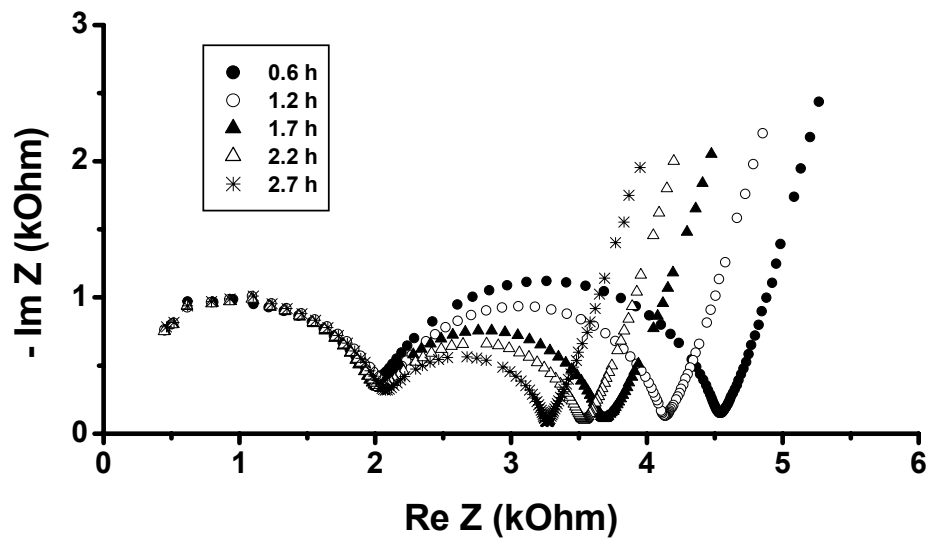


Figure 2: Impedance diagrams, measured at 400 °C in the frequency range 5 Hz - 13 MHz, of $ZrO_2:8\% \text{ mol } Y_2O_3$ sintered at 1350 °C for 0.6 h, 1.2 h, 1.7 h, 2.2 h and 2.7 h .

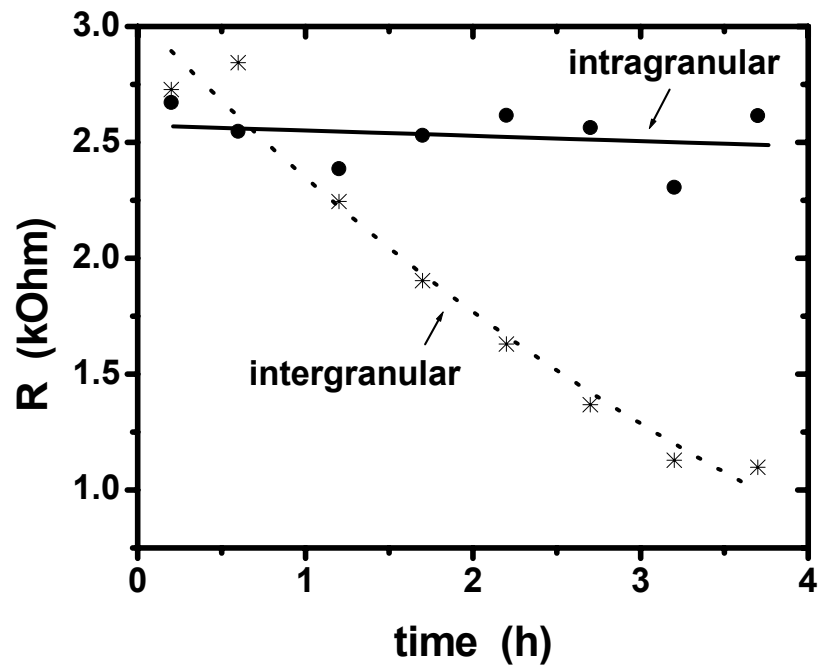


Figure 3: Dependence of the intergranular (grain boundary) and intragranular (bulk) resistance of $ZrO_2:8\% \text{ mol } Y_2O_3$ pellets sintered at 1350 °C (third sintering stage) for different times.

From the impedance diagrams of the ZrO_2 :8% mol Y_2O_3 ceramics sintered at 1350 °C for different times, α_R and α_f were determined. In Fig. 4 the product $\alpha_R \cdot \alpha_f$ is plotted as a function of sintering time. The decrease of that product points to pore elimination, as expected. The higher is the sintering time, the higher is the average grain size at the expenses of pore elimination.

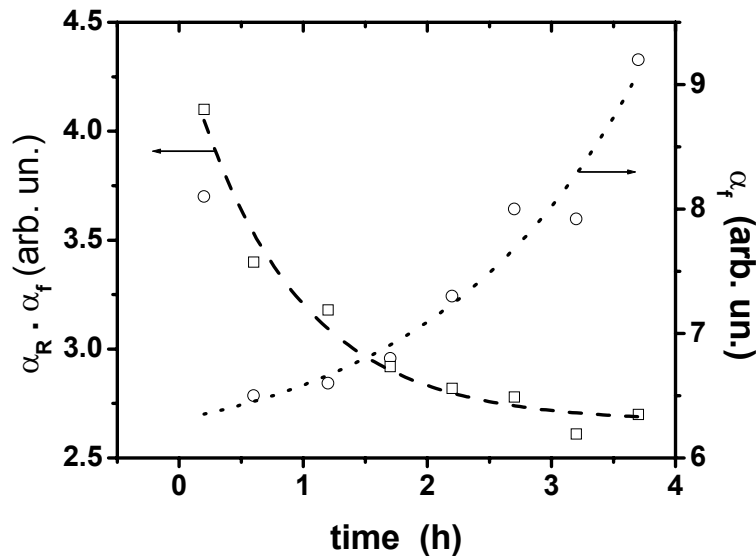


Figure 4: Dependence of $\alpha_R \cdot \alpha_f$ on the sintering time at 1350 °C of ZrO_2 :8% mol Y_2O_3 pellets. α_R : resistance blocking factor, α_f : frequency factor (see text for details).

The temperature of 1367 °C is determined as the one corresponding to reaching about 70% of the theoretical density. The zirconia-8 mol% yttria green pellets were prepared by cold chomping followed by isostatic pressing. All specimens were heat treated at 1367 °C in air inside a tubular furnace. The heating and cooling rates were 20 °C min^{-1} without any dwelling time. The specimens were then subsequently heated at 1300 °C for different period of time (0, 1, 2, 3, 5 and 10 h), two samples for each time. One of each two samples had silver electrodes applied to the parallel surfaces for impedance spectroscopy analysis; the other was polished with diamond paste, heat treated at 950 °C for a short time to reveal grain boundaries without allowing for grain growth, covered with Au-Pd by evaporation under vacuum and observed in the scanning electron microscope. The impedance spectroscopy diagrams are shown in Figure 5. The temperature of measurement was approximately 400 °C in the frequency range 5 Hz - 1 MHz.

One hour of heat treatment at 1300 °C is sufficient for a large decrease in the intergranular resistance R_{gb} . All impedance diagrams had their intergranular and intragranular resistivity values determined by separating both contributions in the frequency domain assuming equivalent R//C circuits for bulk and grain boundary contributions in series (circuits in the inset in Figure 5). Moreover,

the geometrical factor of each pellet and correction for differences in temperature of measurement were taken into account.

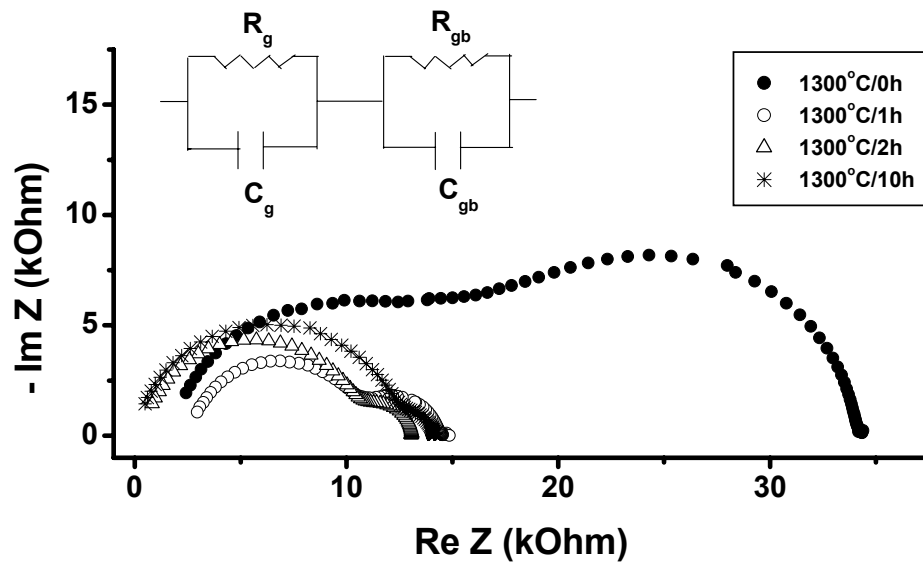


Figure 5: Impedance spectroscopy diagrams of zirconia-8mol% yttria pellets sintered at different times at 1300 °C. Temperature of measurement: 400 °C; frequency range: 10-10⁶ Hz.

The dependence of the grain boundary resistivity on the sintering time at 1300 °C is plotted in Figure 6.

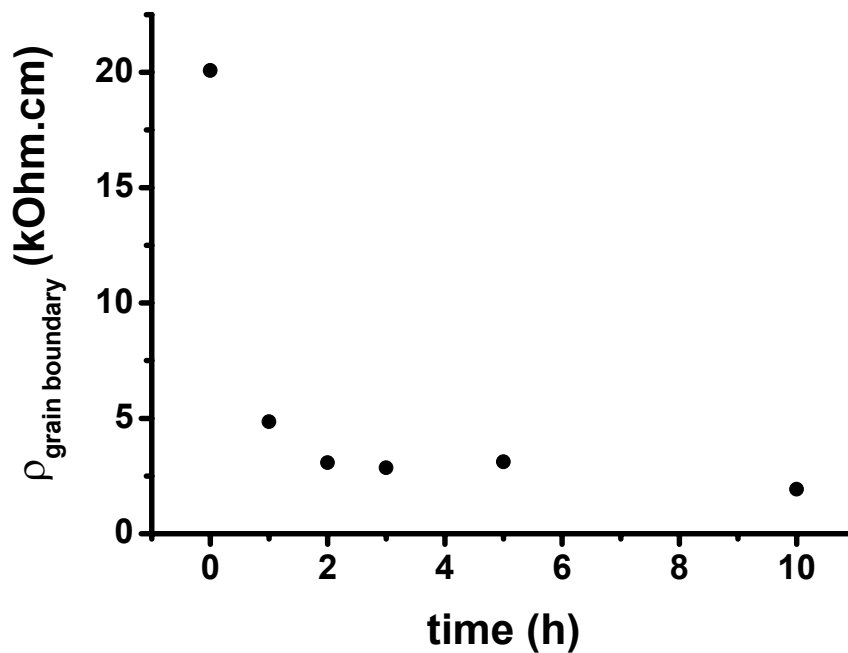


Figure 6: Values of the grain boundary resistivity as a function of the time the specimen ZrO_2 : 8 mol % Y_2O_3 is heat treated at 1300 °C.

Figure 7 shows the corresponding behavior of the average grain size determined after the SEM micrographs, which are shown in Figure 8.

A clear evolution of the average grain size is observed. These images have been analyzed by the intercept method [18] and using available software. The results, with the corresponding statistical deviations, are shown in Table I.

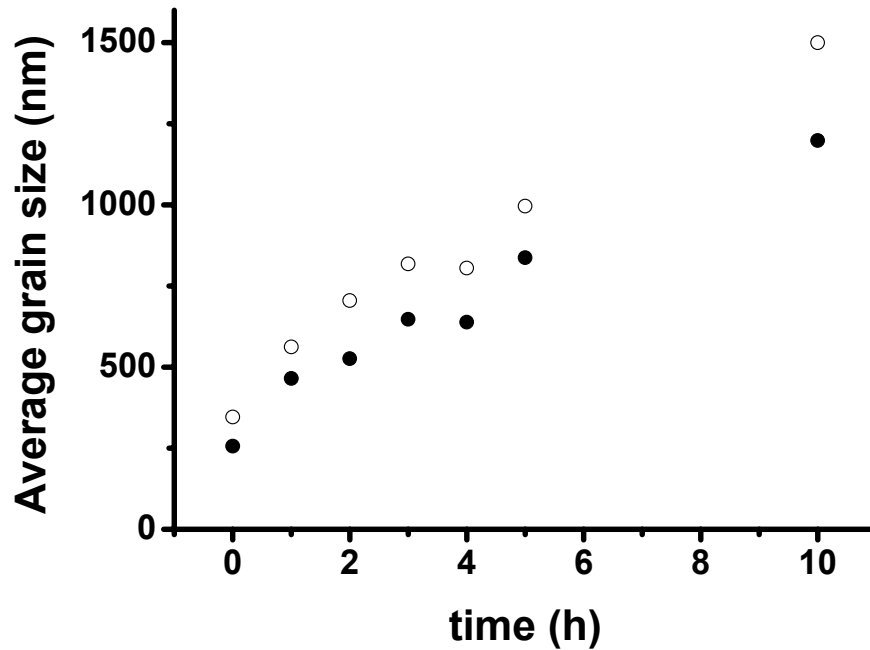


Figure 7: Values of the average grain size of ZrO_2 : 8 mol% Y_2O_3 pellets sintered at different times at 1300 °C. Methods of evaluation of grain size: Mendelson (o) and image analysis software (●).

Table I: Values of average grain size of zirconia-8 mol% yttria

dwelling time at 1300 °C	Average grain size ^a (nm)	Average grain size ^b (nm)
0	346 ± 115	256 ± 190
1	562 ± 108	465 ± 175
2	705 ± 159	526 ± 345
3	818 ± 230	647 ± 390
4	805 ± 267	638 ± 482
5	996 ± 258	837 ± 461
10	1500 ± 287	1198 ± 622

^aMendelson method [23]; ^bImage analysis method

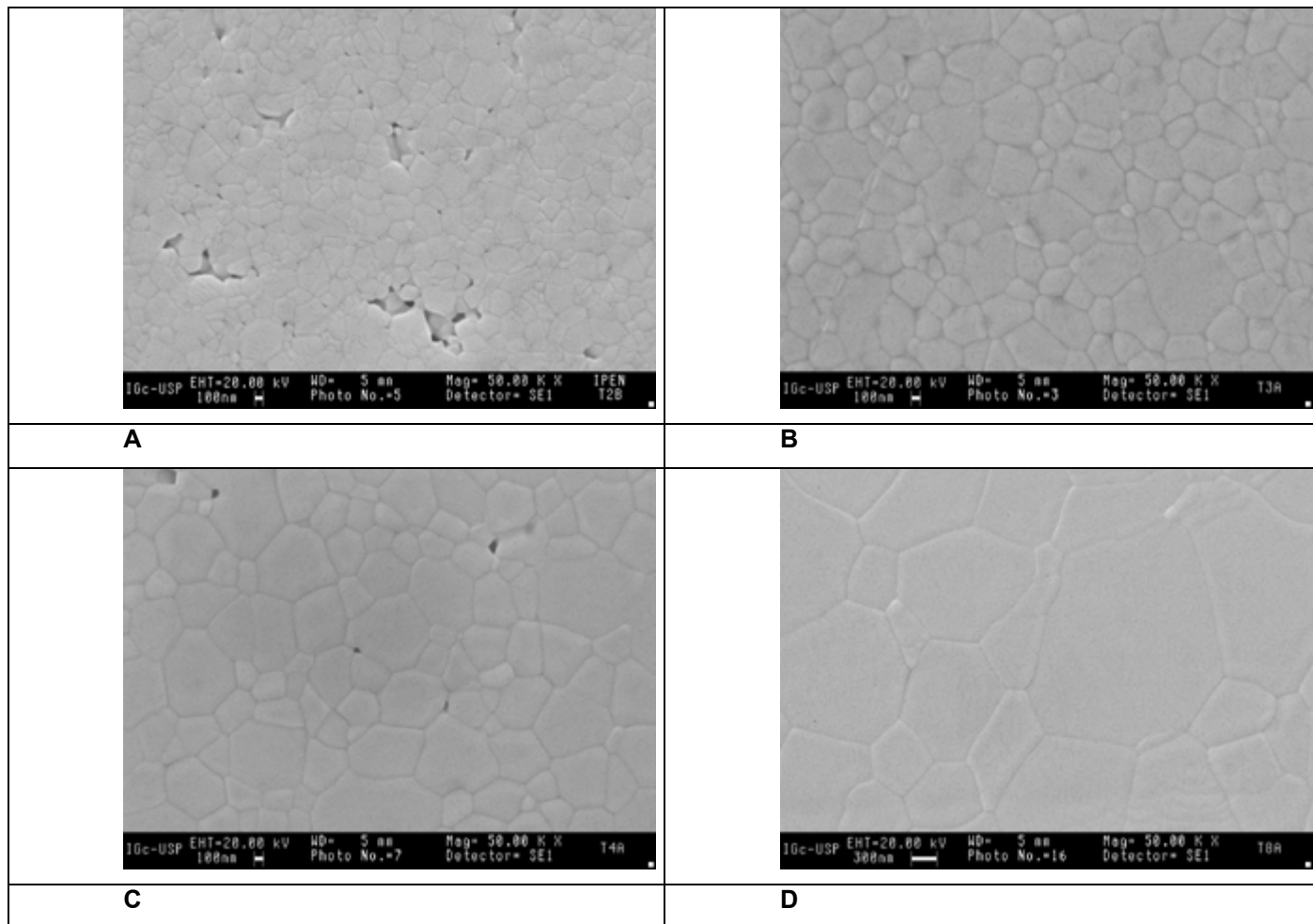


Figure 8: Scanning electron microscope micrographs of zirconia-8 mol% yttria pellets pre-sintered at 1367 °C (first step) and sintered at 1300 °C during 0 h (A), 1 h (B), 2 h (C) and 10 h (D).

Finally, the two-step sintering procedure was repeated for specimens heat treated at 1400 °C / 0.1 h (first step) followed by sintering at 1000 °C for 0 □ t □ 5 h (second step) and also followed by sintering at 1200 °C for 0 □ t □ 5 h (second step). The results are shown in Table 2.

The results presented in Table II are similar to the ones reported in Figure 5: the grain boundary resistivity decreases for increasing sintering times, indicating that the density of grain boundaries decreases, i.e., there is an increase in the average grain size.

Table II: Values of grain boundary resistivity of ZrO₂: 8 mol% Y₂O₃ pellets sintered according to the two-step sintering procedure using different heating profiles.

Heating profile	Temperature of measurement (°C)	ρ_{gb} (10 ⁴ Ohm.cm)
1400 °C / 0.1h + 1100 °C / t		
t = 0 h	295-300	3.5
t = 1 h	295-300	5.8
t = 2 h	295-300	4.3
t = 3 h	295-300	3.9
t = 5 h	295-300	2.6
1200 °C / 0 h + 1000 °C / t		
t = 0 h	464	88
t = 1 h	466	26
t = 2 h	466	95
t = 3 h	465	33
t = 5 h	463	8.4

CONCLUSIONS

The increase in the average grain size of ZrO₂: 8 mol% Y₂O₃ solid electrolytes with nanosized grains was followed by measuring the decrease of the grain boundary resistivity. The two-step sintering process was applied to these electrolytes by heat treating at a temperature corresponding to 70% of their density followed by quenching and heating at different lower temperatures for several periods of time. In agreement with scanning electron microscopy analysis, the decrease in the grain boundary resistivity was always measured with a corresponding increase in the average grain size. Two are the main conclusions: a) the impedance spectroscopy technique proved once more to be a very useful technique for following average grain size variation in ceramic solid electrolytes and, consequently, for studying sintering processes; b) the two-step sintering did not show to be useful for producing zirconia-yttria solid electrolytes dense and with grain sizes as small as the average grain size of the starting powders.

ACKNOWLEDGEMENTS

To CNEN, PRONEX and FAPESP (Proc. 99/10798-0) for financial support. RM and ENSM acknowledge CNPq (Procs. 306496/88-7 and 300934/94-7). DZF acknowledges FAPESP for the post-doctoral scholarship (Proc. 03/08793-8).

REFERENCES

- [1] Aoki, M.; Chiang, Y. -M. ; Kosacki, I. ; Lee, L. J. -R. ; Tuller H. L., Lu, Y. **Journal of the American Ceramic Society**, v. 79, p. 1169, 1996.
- [2] Badwal, S. P. S. ; Drennan, J. **Journal of Materials Science**, v. 22, p. 3231, 1987.
- [3] Bauerle, J. E. **Journal of Physics and Chemistry of Solids**, v. 30, p. 2657, 1969.
- [4] Bernard, H. These, INPG, France, 1980.
- [5] Brook, R. J. In Advances In Ceramics, **Science and Technology of Zirconia**, Heuer, A. H.; Hobbs, L. W. Editors, v. 3, p. 272, Columbus, Ohio: The American Ceramic Society, 1981.
- [6] Chen, I.-Wei ; Wang, X,-H. **Nature**, v. 404, p. 168, March 2000.
- [7] De Florio, D. Z. ; Muccillo, R. **Solid State Ionics**, v. 123, p. 301, 1999.
- [8] Dessemond, L.; Muccillo, R.; Hénault, M.; Kleitz, M. **Applied Physics A**, v. 57, p. 57, 1993.
- [9] German, R. M. **Powder Metallurgy Science**, p.145, Metal Powder Industries Federation, Princeton, 1984.
- [10] Gödickemeier, M.; Michel, B.; Orliukas, A.; Bohac, P.; Sasaki, K.; Gauckler, L.; Heinrich, H.; Schwander, P.; Kostorz, G.; Hofmann, H.; Frei, O. **Journal of Materials Research**, v. 9, p. 1228, 1994.
- [11] Ioffe, A. I.; Inozemtsev, M. V.; Lipilin, A. S.; Perfilev, M. V.; Karpachov, S. V. **Physica Status Solidi (a)**, v. 30, p. 87, 1975.
- [12] Jagannatan, K. P.; Tiku, S. K.; Ray, H. S.; Gosh, A.; Subbarao, E. C. In **Solid Electrolytes and their applications**, Subbarao, E. C. Editor, p.201, New York and London: Plenum Press, 1980.
- [13] Kleitz, M.; Pescher, C.; Dessemond, L. In **Science and Technology of Zirconia V**, Badwal, S. P. S.; Bannister, M. J.; Hannick, R. H. J. Editors, p. 593, Lancaster : Technomic Publishing Company, 1993.
- [14] Kleitz, M.; Dessemond, L.; Steil, M. C. **Solid State Ionics**, v. 75, p. 107, 1995.
- [15] Kleitz, M.; Kennedy, J. H. In Vashishta, P.; Mundy, J.N.; Shenoy, G.K. Editors, **Fast Ion Transport in Solids**, p. 185, Elsevier North Holand, 1979.
- [16] Kleitz, M.; Bernard, H.; Fernandez, E.; Schouler, E. In **Science and Technology of Zirconia I**, Advances in Ceramics, Heuer, A. H.; Hobbs, L. W. Editors, v. 3, p. 310, Columbus, Ohio : The Am. Ceram. Soc., 1981.
- [17] Lee, Y.-Il ; Kim, Y.-W.; Mitomu, M.; Kim, D.-Y. **Journal of the American Ceramic Society**, v. 86, p. 1803, 2003.
- [18] M. I. Mendelson, **Journal of the American Ceramic Society**, v. 52, p. 443, 1969.
- [19] J.-C. M'Peko, A. R. Ruiz-Salvador, G. Rodrigues Fuentes, **Materials Letters**, v. 36, p. 290, 1998.
- [20] Muccillo, R.; Muccillo, E. N. S.; França, Y. V.; Fredericci, C.; Prado, M. O.; Zanotto, E. D. **Materials Science and Engineering A - Structure**, v. 352, p. 232, 2003.
- [21] Shaw, N. J. **Powder Metallurgy International**, v. 21, p. 16, 1989.
- [22] Steil, M. C.; Thevenot, F.; Kleitz, M. **Journal of the Electrochemical Society** v. 144, p. 390, 1997.

[23] Tai, L. W.; Nasrallah, M. M.; Anderson, H. V.; Sparlin, D. M.; Sehlen, S. R. **Solid State Ionics** v. 76, p. 250, 1995.

[24] Verkerk, M. J. ; Middelhuis, B. J.; Burggraaf, A. J. **Solid State Ionics**, v. 6, p. 159, 1982.